Inflow Noise: Prediction and analysis of the relevance for a multi-megawatt turbine

Cordula Hornung[1], Christoph Scheit[2], Nils Noffke[2], Andree Altmikus[2], Thorsten Lutz[1], Ewald Krämer[1]

[1] *Institute for Aerodynamic and Gas Dynamic, University of Stuttgart, 70569 Stuttgart*

[2] *WRD GmbH, 26607 Aurich*

E-Mail:Cordula.Hornung@iag.uni-stuttgart.de

Introduction

In the new European noise guidelines of the WHO, published in October 2018, wind turbine noise was explicitly added to the catalogue of noise sources for which acceptable limits are specified [1]. This points out once more the relevance noise stemming from wind turbines has gained over the years. It is now considered to be one of, if not the most important factor for public acceptance of wind turbines [2]. In the past, different studies have shown that for most sites trailing edge noise (TEN) has the highest contribution to the overall sound power level (SPL) in the audible range. However, more recent studies suggest that depending on the ambient turbulence intensity (TI) level inflow noise (IN) can contribute significantly to the SPL. Another exception where IN gains importance are small wind turbines where TEN is already outside the audible range. Nevertheless, also for large rotors at normal TI levels the lower frequency part of the spectrum originates from IN.

TEN stems from an interaction of the turbulent vortices with the airfoil's trailing edge. The vortices induce wall pressure fluctuations (WPF) which are scattered at the edge and propagate as sound waves to the far field following an edge-noise directivity pattern. IN is generated by the interaction of the blades with the atmospheric turbulence. Similar to TEN it contributes to the broadband noise, however, is characterized by lower frequencies. The directivity pattern of IN depends on the ratio between the length scale of the incoming turbulence and the chord. For large length scales a dipole patters occurs whereas for smaller length this changes to an edge noise directivity.

Because of the importance of noise emissions, reliable prediction methods as well as an understanding of the relevant sources for different observer positions and mechanisms is crucial for wind turbine manufacturers. In literature, different methods to predict noise can be found. Starting with empirical models, over semi-analytical models up to CAA, there is a wide range of different approaches, which are best suited for different applications. The probably best known empirical method is the BPM model, which contains model equations for a variety of noise sources of airfoils [3]. Therefore, it has been used by many manufacturers in the past. Now, there is a shift towards more complex models, due to the increase in available computational power. However, the noise prediction of whole rotors with the help of CAA methods in industrial contexts is still out of reach because of the enormous computational power required. Semi-analytical methods, on the other hand, offer a good compromise. They are often combined with the CFD calculations, which are integrated as standard in modern product development cycles.

Within the present study the wind turbine noise prediction code IAGNoise+ is used. It is developed at the Institute of Aerodynamics and Gas Dynamics (University of Stuttgart) and employs semi-analytical methods for wind turbine's noise prediction. It already included a TEN model [4] and is extended and validated for an IN model in the framework of this research. Afterwards, IAGNoise+ is used to evaluate the influence of TEN and IN for different observer positions. The study is conducted using a prototype design of a multi-megawatt Enercon turbine.

The paper is structured as follows: The implemented models as well as the measurement methods are described in the methods section. Subsequently, the comparison between measurement and prediction and the results for different observer positions are presented and discussed. Finally the findings are summarized and a short outlook is given.

Methods

Measurements

The noise measurements presented here were carried out in the framework of an extensive measurement campaign from Enercon GmbH between September 2017 and March 2018. During this time two microphones were located downstream of the prototype turbine at the same distance but different angles. The third-octave band data from 20 Hz to 6.3 kHz was measured in 10 s intervals. Thereby, the noise levels were corrected for the levels during standstill – a cyclic shutdown concept was used with 1h 40 min operation alternating with 20 min standstill. Only noise levels, which exceeded the standstill levels by 3 dB or more were taken into account. For the evaluation of the noise, only audio data is used in which the microphones were located at +/- 15° with respect to the direct wake of the turbine. In addition, a wind met mast was installed upstream of the turbine. It measured the wind speed and directions as well as the velocity fluctuations in mean flow direction at different heights above ground (37 m, 63 m, hub height =98 m, 99 m). From the data the turbulence intensity (TI) used in the prediction of noise is determined with a sliding window. The 10 min windows (600 values at 1 Hz) for this calculation were placed symmetrically around the 10 s acoustic data points as far as possible. Then, the measured sets are binned according to the TI as well as with respect to the rpm of the turbine.

According to [5] the length scale of the energy-containing eddies Λ can be either determined from the measurements via:

$$\Lambda \approx \frac{\sigma_u}{dU/dz}$$

or by

$$\Lambda \approx \frac{z\,\sigma_u}{U\,\alpha}. \qquad (0.1)$$

In this equation σ_u is the variance of the measured fluctuations, dU/dz is the gradient of the mean wind speed U over the height z and α the shear exponent. Within this research Λ is first evaluated with both approaches at different

heights. The value for the prediction is then determined based on a third order regression for all points.

Prediction of Inflow Noise

The inflow noise is predicted within IAGNoise+ using the model developed by Patterson and Amiet [6]. The theory includes the effects of compressibility and non-compactness, but ignores end effects [7]. By regarding turbulence as a random quantity and thus applying statistical measures such as cross-power spectral densities (PSD) an equation for the far field noise produced by inflow turbulence can be derived. It uses the theory developed by Kirchhoff and Curle by which the cross-PSD of the wall pressure fluctuations can be related to the emitted far field noise [6]. This relation can be simplified for acoustics wavelengths being much smaller than the airfoil semi-span. For this assumption the airfoil loading becomes concentrated within an order of wavelength from the LE and finite span effects are limited to distances of the same order of magnitude [7]. This finally leads to the here used model equation (0.2) for the two sided far field noise spectrum $S_{pp}(\boldsymbol{r},\omega)$. To compare the inflow noise prediction with measurements a conversion to a physical realizable one sided spectrum is necessary.

$$S_{pp}(\boldsymbol{r},\omega) = \left(\frac{\omega z \rho_{ref} c}{4 c_0 \sigma^2}\right) \pi U_1 L \left|\mathcal{L}(\boldsymbol{r},K_x,K_y)\right|^2 \Phi_{ww}(K_x,K_y) \quad (0.2)$$

$$with: K_x = \frac{\omega}{U_1} \; and \; K_y = \frac{\omega y}{c_0 \sigma}$$

In equation (0.2) ω represents the frequency, ρ_{ref} the density, c the chord length and c_0 the speed of sound. The x axis is oriented in the direction of the mean flow U_1, y in wall normal and z in span wise direction. The inflow turbulence spectrum is described by Φ_{ww} and $\boldsymbol{r}$ is the vector towards the observer. σ is the observer distance scaled for compressibility effects by applying the Prandtl-Glauert correction β. The effective lift $\mathcal{L}$ is calculated based on the airfoil response function. It is highly dependent on the ratio between the size of incoming gusts and chord length. Thus, one response function for low frequencies and one for higher frequencies is given. The switching frequency is determined based on the non-dimensionalised parameter μ.

$$\mu = \frac{M K_x c}{2\beta^2} \quad (0.3)$$

For the low frequency regime, i.e. $\mu < 0.4$, a solution for the airfoil lift $\mathcal{L}(\boldsymbol{r},K_x,0)$ is used which is based on an approximation of the Sears function $S(\overline{k_x^*})$. It is correct for $\mathcal{O}(\mu)$ but neglects terms of $\mathcal{O}(\mu^2)$ and higher:

$$\left|\mathcal{L}(\boldsymbol{r},K_x,0)\right| = \frac{1}{\beta}\left|S(\overline{k_x^*})\right|$$

$$with \;\; \overline{k_x} = \frac{0.5}{\beta^2} \cdot K_x \cdot c \quad (0.4)$$

For the high frequency regime, i.e. $\mu > 0.4$, a series of corrections is made for the response function alternatingly for LE and TE. The expression for the effective lift can then be calculated as the sum of the corrections. Here, the first two element of the series are used: $\mathcal{L} = \mathcal{L}_1 + \mathcal{L}_2$ with

$$\mathcal{L}_1(\boldsymbol{r},k_x,0) = \frac{1}{\pi}\sqrt{\frac{2}{(1+Ma)\overline{k_x}H_1}}E^*(2H_1)e^{iH_2} \quad (0.5)$$

and

$$\mathcal{L}_2(\boldsymbol{r},k_x,0) = \frac{i(1-e^{-i2H_1})}{\pi H_1\sqrt{2\pi(1+Ma)\overline{k_x}}}e^{iH_2} + \frac{(1-i)}{\pi H_1\sqrt{2\pi(1+Ma)\overline{k_x}}}e^{iH_2} \cdot \left[E^*(4\mu) - \sqrt{\frac{2}{1+\frac{x}{\sigma}}}\, e^{-i2H_1}E^*\left(2\mu\left(1+\frac{x}{\sigma}\right)\right)\right] \quad (0.6)$$

In eq. (0.5) and (0.6) $E^*(x)$ represents a combination of Fresnel integrals. The remaining quantities are defined as $H_1 = \mu - \mu x/\sigma$ and $H_2 = \overline{k_x^*}\,(1 - Ma\,x/\sigma) - \pi/4$.
The inflow spectrum is modeled assuming an isotropic two-dimensional van Karman spectrum:

$$\Phi_{ww}(k_x,k_y) = \frac{4}{9\pi}\frac{u_{rms}^2}{k_e^2}\frac{\hat{k}_x^2+\hat{k}_y^2}{\left(1+\hat{k}_x^2+\hat{k}_y^2\right)^{\frac{7}{3}}} \quad (0.7)$$

$$with \;\; \hat{k}_i^2 = \frac{k_i^2}{k_e^2}$$

k_e is the wavenumber of the energy containing eddies and can be determined based on the length scale from the measurements with $k_e = 1/\Lambda$.. The original model as developed by Paterson and Amiet [7] had a quite good prediction quality for high Ma numbers, however, as already shown in their publication, deviated significantly from measurements for lower Ma. This deviation originates in their flat plate assumption. In the Ma number rage of operating wind turbines these thickness effects are, however, significant. A literature research revealed two different thickness correction methods. Both methods were determined by empirical fitting approaches. The thickness correction by Tian et al. [8] was developed based on measurements of a NACA0012. Moriarty et al. [9] utilized a quite extensive test matrix with different airfoil geometries including chambered and non-chambered airfoils as well as different LE radius to derive their sound pressure level correction. For a NACA0012 airfoil in a wind tunnel the two methods lead to very similar results. However, as shown in this paper this changes for wind turbines.

Prediction of TE Noise

The TEN is also predicted using the in-house code IAGNoise+. It employs an enhanced TNO-type model [10, 11].The principal procedure follows three steps: First, the boundary layer characteristics close to the TE are gained from RANS CFD simulations. With these parameters the power spectral density of the WPF is predicted. Finally, they are used as input to the far field model equation. The main difference to the TNO model by Parchen [11] is that in the here used model the interaction between the turbulent vortices in the boundary layer is taken into account. Therefore, a reliable prediction of TEN also for high angles of attack up to slight TE separation is feasible. Further differences include the model for the moving axis spectrum and the consideration of anisotropy. For the latter, the approach developed by Kamruzzaman [12] is used, but was extended to include the influence of the pressure gradient. For detailed information on the employed model and modeling parameters the reader is referred to [10] and [4].

The CFD simulations for the TEN prediction were performed by M. Arnold (Enercon), using the compressible structured CFD-solver FLOWer, developed by the German Aerospace Center (DLR). The simulation was conducted

fully turbulent, using the two equation Menter SST k-ω model. This corresponds to the surface soiling on the blade acting as tripping mechanism. The simulation domain is constricted to a single blade 120° mesh. In total, the setup consists of 17 mio. cells in 236 blocks. The boundary layer grid is set up to achieve a y+ value of approximately 1 of the first cell row on the rotor blade's surface with an expansion factor of 1.1. As far field boundary condition uniform inflow was applied, neglecting possible shear or TI.

Results and Discussion

In the Atmospheric Boundary Layer (ABL) a variety of different influences determine its current state. Depending on velocity and temperature gradient it behaves differently. Because of this, it is very challenging to obtain measurement points at constant conditions. Since turbulence generation is a particularly fast changing mechanism, the data gained during the measurements are relatively widespread. In figure 1 the third-octave noise levels at 50 Hz are depicted for different measurement points at a rpm of 15.2. They are plotted over the turbulence intensity (TI) and colored by the shear exponent determined between 98 m and 63 m. It stands out that for a distinct TI the noise levels are scattered over a range of about 8 dB. For higher frequencies – related to TEN – the spectra collapse (cf. figure 2). In addition, figure 1 shows that TI changes with the shear exponent. Higher shear corresponds to a faster decay of eddies and thus smaller eddy sizes (= smaller length scales) and most times lower TI.

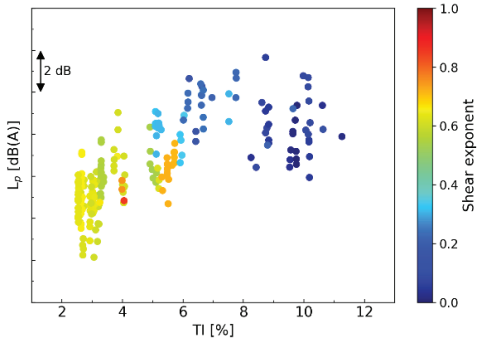

Figure 1: Noise levels at 50 Hz for different TI for 15.2 rpm.

The input parameter for the IN prediction code are determined from of the wind met mast measurements. The length scales are first calculated for all shear exponents measured with both methods in eq. (0.1) since they are very sensitive towards slight changes in velocity gradient or shear. Subsequently a third order regression is defined which is then used to determine the corresponding length scales for the prediction method. Within this paper, results for three different TI are evaluated. An overview over the TI and the related length scales is given in Table 1.

Tabelle 1: Input parameter for prediction.

	15.2 rpm			14.5 rpm
TI [%]	2.8	5.5	10.1	10.0
Λ[m]	6.23	6.05	39.08	8.87

The results are shown in figure 2. Depicted are all measured spectra with symbols, in comparison with predictions without correction (solid line) and with the correction of Moriarty (dashed-dot-lines). In the diagram, each color represents one TI, with a shift of 10 dB in between for better distinction.

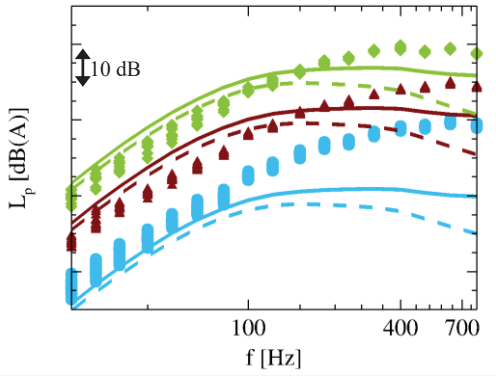

Figure 2: Measured (symbols) and predicted inflow noise spectrum (15.2 rpm). With thickness correction Moriarty: dashed-lines, without: solid lines, for TI=10.1% (◆), TI=5.5% (▲), TI=2.8% (●), (shift of 10 dB between each TI).

The measured spectra are corrected for effects of a completely sound reflecting measurement plate, according to the IEC61400-11 by subtracting 6 dB. While this is valid for the high frequencies, there are some doubts about this assumption in the lower frequency range. Thus, the shown spectra are probably slightly higher in reality. Comparing measurements and predictions for a TI of 10.1%, below 100 Hz the predictions match the measurements quite well. With the correction on Moriarty the predicted noise levels are slightly smaller for the lower frequencies and decrease faster towards the higher frequencies. The correction proposed by Tian et al. has, in contrast to 2D, no effect in 3D. The corresponding curve is located beneath the uncorrected line for all cases. Also for a TI of 5.5% the IN levels are predicted well. In particular, the difference in sound pressure levels for the two different TI is captured. The lowest TI shown is 2.8%. In contrast to the higher TI the measured spectrum is under-predicted by IAGNoise+. The reason for this is assumed to be the isotropic van Karman spectrum which is used to model the inflow turbulence. While this is a fair approximation for high TI flows in the ABL or wind tunnels, it does not depict the characteristics in low TI wind. With higher shear coefficients, related to low TI, the anisotropy of the turbulence increases fast. Thus, the error because of the anisotropy is neglected increases for lower TI. For higher frequencies the predicted IN spectrum deviates from the measurements as expected, since TEN dominates the overall spectrum for this range.

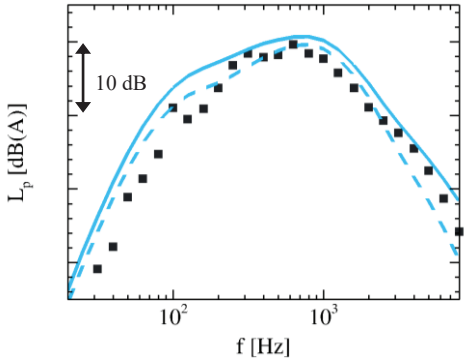

Figure 3: Measured (■) and predicted noise spectra at 14.5 rpm for IN and TEN at, with thickness correction by Moriarty: dashed-lines, without: solid line.

This is further supported by figure 3, which compares measured and predicted IN and TEN for a different operation point at 14.5 rpm and measured at a different time

of the year. During these measurements a different generator was installed in the turbine, which emitted a tonal sound, resulting in the 100 Hz hump in figure 3's measured spectra. As in figure 2, the predicted spectrum with and without correction by Moriarty is plotted. When looking at the uncorrected spectrum, it can be concluded that with the combination of TEN and IN it is possible to predict the measured noise level over the complete audible frequency range. Similar to the above shown results, the frequency range of the inflow noise is slightly over predicted (equal to the previous measurements the correction for the sound-reflecting plate was applied). However, the correction proposed by Moriarty increases the prediction quality.
In a last step, IN and TEN immission are compared. Taking directivity and distance effects into account, but neglecting reflection, deflection and absorption of the sound waves, the overall sound pressure levels for both sources are determined. The results are shown in figure 4 for different observer positions around the turbine, at four distinct radial distances.

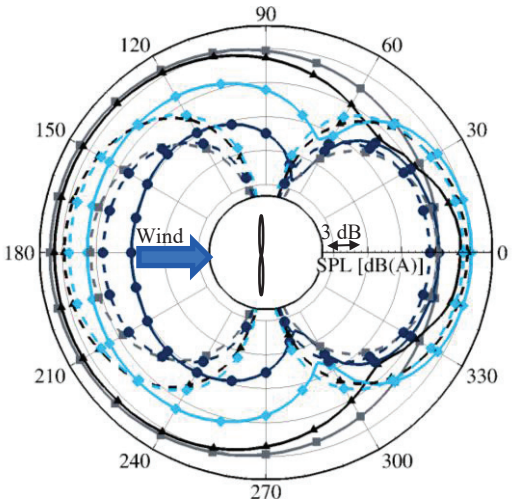

Figure 4: TEN (solid lines) and IN (dashed lines) at the ground for radial distances of 27% ( ), 49% ( ), 114% ( ) and 21% ( ) of the rotor diameter for Ti=10% and 14.5rpm.

The TEN level exceeds the IN level over most of the area, but in particular in the cross wind direction. At the IEC 61400 measurement position downwind of the turbine the TEN noise is still higher than the IN noise. However, at large distances upstream of the turbine the IN is higher than the TEN.

Conclusions

The paper presents a prediction approach for the two main aeroacoustic mechanisms – trailing edge noise (TEN) and inflow noise (IN) - at wind turbines. With the methods it is possible to predict the complete audible spectrum. For low turbulence intensity (TI) the measurements were under predicted whereas for high TI the prediction matched the measurements or slightly over predicted it. A comparison between the TEN and IN immission revealed that far away upstream of the turbine the IN immission is higher than the TEN immission for this case. Future work on this topic should include the implementation of an anisotropy model to improve the prediction quality in particular for low turbulence intensities.

Acknowledgments

This research is funded by the BMWi within the framework of the German joint research project Schall_KoGe (Grant number: 0324337C). Thanks goes to M. Arnold from Enercon GmbH for conducting the evaluated CFD simulation.

Literature

[1] World Health Organisation , "Environmental Noise Guidelines for the European Region," 2018.

[2] J. Rand and B. Hoen, "Thirty years of North American wind energy acceptance research: What have we learned?," *Energy Research and Social Science,* February 2017.

[3] T. Brooks, D. Pope and M. Marcolini, "Airfoil Self-Noise and Prediction," *NASA Reference Publication,* vol. 33, no. 6, pp. 1-8, 1989.

[4] C. Hornung, C. Scheit, C. Napierala, M. Arnold, D. Bekiropoulos, A. Altmikus and T. Lutz, "Predicted and Measured Trailing-Edge Noise Emission for a 2.3 MW Wind Turbine," in *7th International Conference on Wind Turbine Noise* , Rotterdam, 2017.

[5] M. Kelly, "From standard wind measurements to spectral characterization: turbulence length scale and distribution," *Wind Energy Science,* 2018.

[6] R. K. Amiet, "Acoustic Radiation from an Airfoil in a Turbulent Stream," *Journal of OSund and Vibration,* no. 41 (4), pp. 407-420, 1975.

[7] R. W. Paterson and R. K. Amiet, "Noise and Surface Pressure Response of an Airfoil to Incident Turbulence," *J. Aircraft,* vol. Vol 14, August 1977.

[8] Y. Tian, B. Cotte and A. Chaigne, "Wind Turbine Noise Modelling Based on Amiet' s Theory," in *5th International Meeting on Wind Turbine Noise*, Denver, CO, United States, 2013.

[9] P. J. Moriarty, G. Guidati and P. Migliore, "Prediction of Turbulent Inflow and Trailing-edge Noise for Wind Turbines," in *11th AIAA/CEAS Aeroacoustics Conference*, Monterey, 2005.

[10] C. Hornung, T. Lutz and E. Krämer, "A model to include turbulence-turbulence interaction in the prediction of trailing edge far field noise for high angle of attack or slightly separated flow," *Renewable Energy, vol. 136, pp 945-954 ,* 2019.

[11] R. Parchen, "Progress report DRAW: a prediction scheme for trailing edge noise based on detailed boundary layer characteristics.," *TNO Institute of Applied Physics, The Netherlands,* 1998.

[12] M. Kamruzzaman, D. Bekiropoulos, A. Wolf, T. Lutz and E. Krämer, "Rnoise: A RANS based airfoil trailing-edge noise prediction model.," *AIAA2014-3305, Atlanta,,* 2014.

[13] Y. Tian and B. Cotte, "Wind Turbine Noise Modeling Based on Amiet's Theory: Effects of Wind Shear and Athmospheric Turbulence," *Acta Acustica united with Acustica,* vol. 102, pp. 626-639, 2016.